Polymer Degradation and Stability 169 (2019) 108954

Contents lists available at ScienceDirect

Polymer Degradation and Stability

journal homepage: www.elsevier.com/locate/polydegstab

TG-MS-FTIR study on pyrolysis behavior of phthalonitrile resin

Bo Liang, Jianbo Wang, Jianghuai Hu, Chengfeng Li, Renke Li, Yao Liu, Ke Zeng*, Gang Yang**

State Key Laboratory of Polymer Materials Engineering, College of Polymer Science and Engineering, Sichuan University, Chengdu, 610065, PR China

ARTICLE INFO

Article history:
Received 10 May 2019
Received in revised form
26 August 2019
Accepted 29 August 2019
Available online 12 September 2019

Keywords:
Phthalonitrile resin
TG-MS-FTIR
Thermal pyrolysis

ABSTRACT

This study firstly reports the thermal pyrolysis behavior of phthalonitrile resin under argon atmosphere. The thermal stability and volatile products analysis were investigated by thermogravimetry coupled with Fourier transform infrared spectroscopy and mass spectrometry (TG-MS-FTIR). It is found that the main gas species detected were H_2O, NH_3, HCN, CH_4, CO_2, CO. In addition, the most probable pyrolysis mechanism was intensively discussed, proposing that the pyrolysis process of PN resin can be divided into two main stages. Firstly, the labile bonds removal from matrix. Secondly, the thermally stable chars in bulk were generated during pyrolysis process.

1. Introduction

High-performance polymers such as epoxy resins and polyimide resins are widely used for a variety of fields, including aerospace industry and microelectronics, due to their excellent properties [1,2]. High-performance materials are characterized by specific criteria, such as long-term durability (>10,000 h) at 177 °C, thermal decomposition temperature >450 °C, high aromatic content and relatively rigid segments that impart high glass transition temperature (T_g) (>200 °C) and high mechanical properties [3]. Accordingly, phthalonitrile (PN) resins are considered to be a class of high-performance materials due to their superior thermal and thermal oxidative stability, high glass transition temperature (T_g), excellent mechanical properties and good moisture resistance [4–10]. In addition, PN resins are commonly used as flame retardant materials because of its low smoke and high carbon residue [11–13]. Based on the advantages above, PN resins are used in a wide range of applications: composites matrix, adhesives, flame retardant materials and carbon precursors [14,15].

The phthalonitrile monomers can be thermally crosslinked in the presence of effective additions such as phenols, benzimidazole, hydrogen imide and organic amine by the formation of triazine ring and phthalocyanine ring to produce void-free thermosets with high crosslinking density [16–19]. And the heterocyclic macromolecular structure of the highly crosslinked PN resin makes it unique in terms of the thermal stability. As is well-known, the thermal stability of high-performance polymer at high service temperatures are always of primary concern. Large amount of literatures focused on investigating thermal behavior of PN resin at high temperature to meet the requirement of high-tech fields. Li et al. [20] investigated the thermal stability of phthalonitrile polymer and phthalonitrile-polyhedral oligomeric silsesquioxane (POSS) copolymer after sintering 3 h at 500 °C, 600 °C and 800 °C. The results suggested that phthalonitrile-polyhedral oligomeric silsesquioxane copolymers have better thermal stability than phthalonitrile polymers. Liu et al. [21] reported a detailed research on the thermal stability of three novel series of soluble and curable phthalonitrile-terminated oligometric poly(ether imide)s containing phthalazinone moiety. It was suggested that the crosslinked polymers showed superior thermal stability with the 10% weight loss temperatures ranging from 543 °C to 595 °C. In our previous work, we studied the pyrolysis kinetics of PN resin at the temperature between 300 °C and 800 °C, and drew the conclusion that the whole thermal pyrolysis of PN resin was following multiple pyrolysis mechanism [22].

TG-MS-FTIR technique is widely used to evaluate the degradation products and gather information about the thermal pyrolysis mechanism. This technique can provide useful information so as to investigate the detailed thermal pyrolysis reactions along with the polymer stability and toxic volatile products under controlled conditions [23]. In literatures there are some studies including TG-

* Corresponding author.
** Corresponding author.
E-mail addresses: zk_ican@sina.com (K. Zeng), yanggang65420@163.com (G. Yang).

https://doi.org/10.1016/j.polymdegradstab.2019.108954
0141-3910/

MS-FTIR analysis for polymer samples such as rigid polyurethane foam [24], polyimide-polydimethysiloxane copolymers [25]. The corresponding study provide a very starting point of the theoretical foundation for accurate prediction of polymer thermal resistance [26].

In this work, TG-MS-FTIR technique was firstly employed to analyze the volatile compounds during the pyrolysis of PN resin. The thermal pyrolysis mechanism of PN resin was presented by combining the analysis results of evolved gas products. In response to the thermal analysis, polymer structures can be rationally designed based on pyrolysis mechanism in order to further improve thermostability.

2. Experimental

2.1. Materials

4-Nitrophthalonitrile (99 wt%) was purchased from Hong Kong's Ming Tai Prosperity Chemical Co., Ltd. Resorcinol (99.5 wt%). Dimethyl sulfoxide (DMSO, AR), acetic acid, K_2CO_3, THF, toluene, acetone and ethanol were supplied by Chengdu Kelong Chemical Reagent Co., Ltd Chengdu, China. All solvents were used as received without further purification.

2.2. Synthesis of self-promoted hydroxy-containing phthalonitrile systems

The monomers of 1, 3-bis(3, 4-dicyanophenoxy)benzene (BDB) and 4-hydroxyphenoxy phthalonitrile (HPPH) are shown in Scheme 1. Synthesis, characterization and proposed polymerization mechanism of self-promoted hydroxy-containing phthalonitrile systems were discussed in previous paper [27].

2.3. Instruments and measurements

On-line testing of gaseous products obtained during the thermal pyrolysis was performed using a thermogravimetric analyzer (NETZSCH STA 449F3 Germany) coupled with a Fourier transform infrared spectrometer (Bruker Tensor 27 Germany) and a mass spectrophotometer (NETZSCH QMS 403 Germany). About 10 mg sample was placed in alumina crucible of TGA and heated from the room temperature to 800 °C at a heating rate of 5, 10 and 15 °C/min under high purity argon atmosphere with the gas flow of 50 ml/min. The connections for gas transportation between the apparatuses were set at 200 °C to prevent condensation of the evolved gases. The spectra for volatile evolution during PN resin pyrolysis can be recorded by means of the Fourier transform infrared spectrometer real-time tracking mode with the scanning range from 4000 cm^{-1} to 650 cm^{-1}. The spectrum scan frequency was 32 times per minute at the resolution of 4 cm^{-1}. The mass spectrometer works in two scanning functions, including full scanning mode and selected ion recording (MID) mode. The MS signals of all the fragment ions (m/z 1–160) were detected by the former mode. The MID mode tracked MS signals of some specific ions marked accurately like m/z 16, 17, 18.

3. Results and discussion

3.1. Thermal analysis of sample

The experimental TGA and DTG curves at 5, 10 15 °C/min are shown in Fig. 1. It is obvious that the pyrolysis of sample was in the

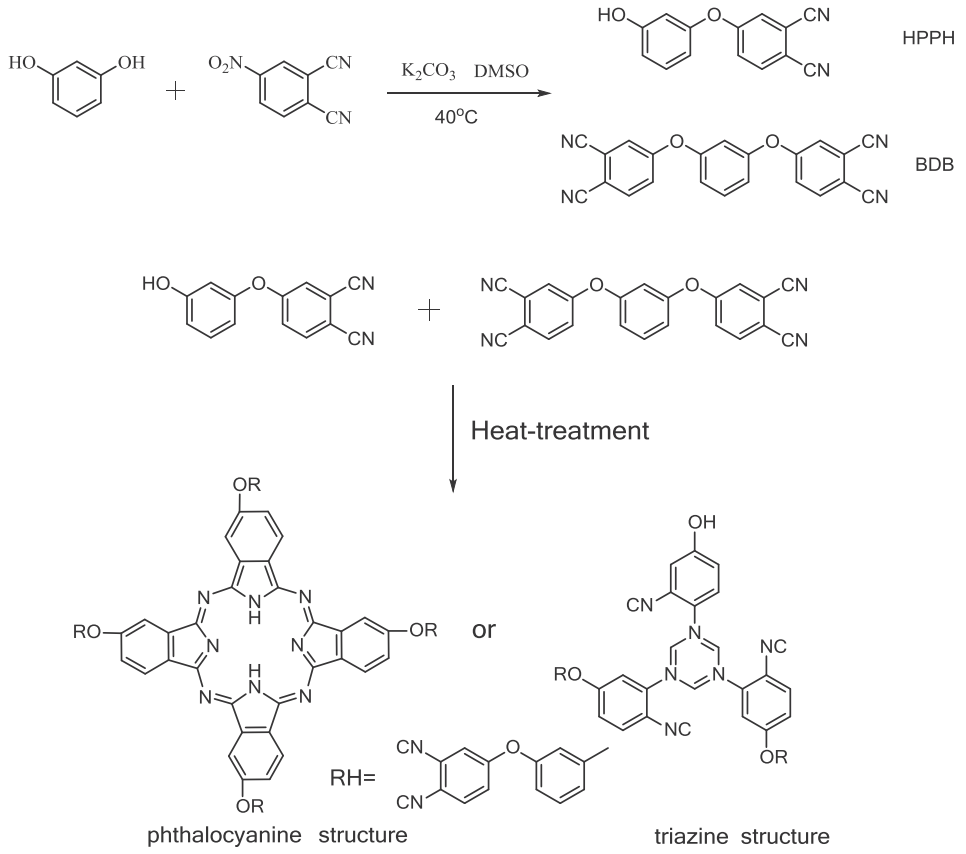

Scheme 1. The monomers of HPPH and BDB and its polymer.

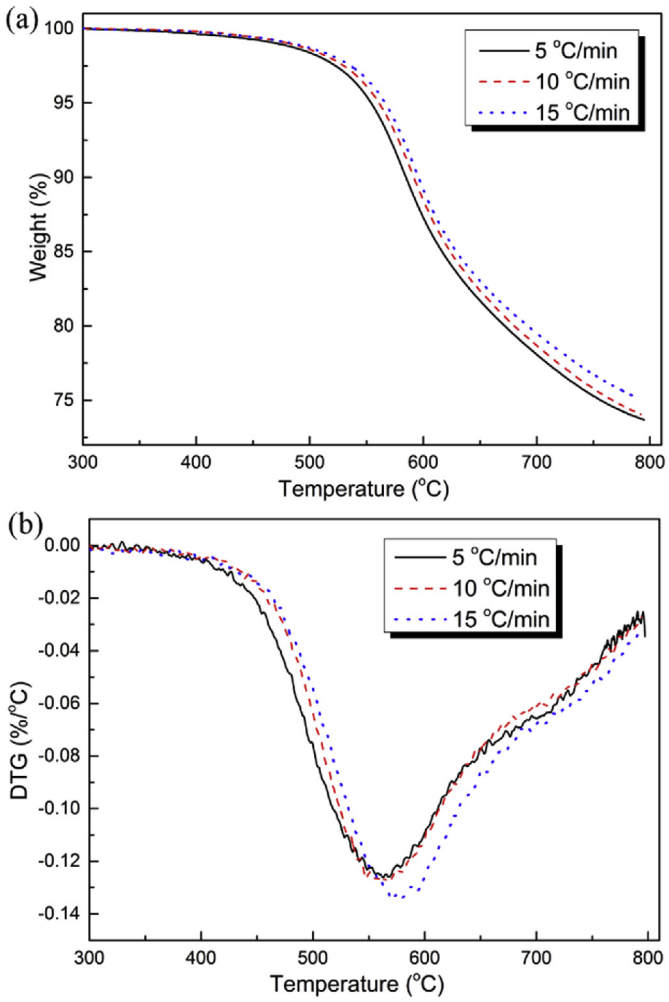

Fig. 1. TG/DTG curves of phthalonitrile resin with different heating rates of 5, 10, 15 °C/min.

range of 450 °C–800 °C from the TGA curves and the decomposition curves shifts to higher temperatures as the heating rate was increased. The corresponding characteristic parameters of the TGA and DTG curve at different heating rates are listed in Table 1. PN resin has excellent thermal stability with the initial pyrolysis temperature at 450 °C. As can be seen in Fig. 1, the DTG curve is asymmetrical and can obviously be divided into several different stages [28]. Therefore, origin 8.5 software was employed to separate the overlapped peaks by using the bi-Gauss multi-peak fitting method. The result indicated that the pyrolysis process of PN resin can be divided into two main stages with respect to temperature (Fig. 2). The characteristic values of each peak are tabulated in Table 2. As shown in Fig. 2 and Table 2, the first pyrolysis stage was spread from 450 °C to 650 °C with the peak at about 560 °C. The second pyrolysis stage was visible from 500 °C to 800 °C with the peak at about 690 °C.

Table 1
Characteristic data of thermal pyrolysis at different heating rates in argon atmosphere.

Heating rates (°C/min)	T_{onset} (°C)	$T_{d\ max}$ (°C)	T_{d5} (°C)	T_{d10} (°C)	T_{d20} (°C)
5	448	579	524	563	664
10	450	580	530	571	677
15	453	582	534	575	688

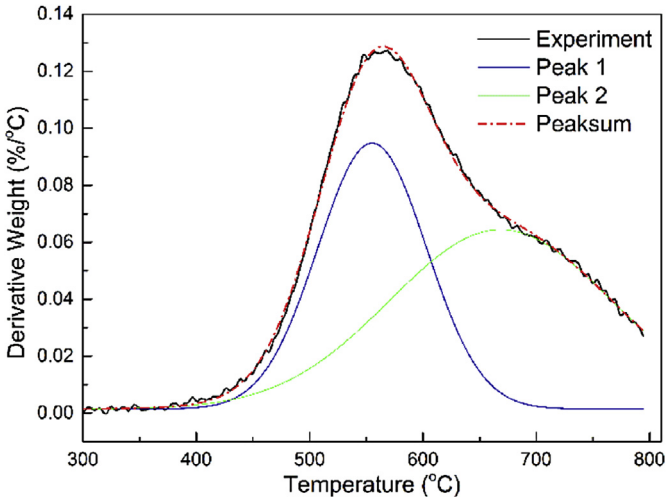

Fig. 2. Deconvolution for DTG curve of 10 °C/min.

T_{onset}, onset degradation temperature, °C; $T_{d\ max}$, temperature corresponding to the maximum weight loss rate, °C; T_{d5}, the temperature at which the weight-loss was 5%, °C; T_{d10}, the temperature at which the weight-loss was 10%, °C; T_{d20}, the temperature at which the weight-loss was 20%, °C;

3.2. TG-FTIR analysis of gas products

The 3D FTIR diagram of PN resin thermal pyrolysis with the heating rate of 10 °C/min is shown in Fig. 3. The remarkable characteristic infrared absorbance band with the highest absorbance at 2360 cm^{-1} is clearly observed. To further recognize the difference of volatiles, the 2D FTIR spectra of gaseous products at several representative temperatures corresponding to the infection points at the TG-DTG curves are shown in Fig. 4, and the main typical bands are listed in Table 3. As is shown in Fig. 4(1), the characteristic bands at 2400-2240 cm^{-1} with peak wavenumbers of 2360 cm^{-1} and 2310 cm^{-1} corresponding to the asymmetric stretching vibrations of carbonyl (C=O) [31]. Weak spectrum band at 1600-1450 cm^{-1} suggests the presence of aromatic ring (skeleton stretching vibrations of aromatic ring C=C) [24]. The remarkable spectrum band at 966 cm^{-1} (N–H bending vibration) and 3340 cm^{-1} (N–H stretching vibration) showed the presence of NH_3, 714 cm^{-1} (C–H bending vibration) and 3312 cm^{-1} (N≡CH stretching vibration) suggested the presence of HCN. [33–35]. Fig. 4(2) presents FTIR spectrum at 563.3 °C that characterizes the most remarkable DTG peak in Fig. 1. Furthermore, 563.3 °C can also be considered as the peak temperature of the first pyrolysis stage according to Fig. 2. Compared with Fig. 4(1), the characteristic bands of CO_2 (2400-2240 cm^{-1}) [31], CO (2230-2050 cm^{-1}) [32] and the C=C stretching absorption from aromatic ring (1600-1450 cm^{-1}) become more clearly. In addition, the absorption band of 4000–3500 cm^{-1} indicated the release of H_2O [29]. The bands at 3400-3250 cm^{-1} are due to N–H stretching vibration [34]. Fig. 4(3) presents FTIR spectrum at 690 °C that corresponding to the peak temperature at second pyrolysis stage in Fig. 2. Compared with Fig. 4(2), the sharply weakened bands of CO_2 and NH_3 are observed in Fig. 4(3). Meanwhile, the band at 3015 cm^{-1} indicates that CH_4 is produced at higher temperature probable due to pyrolysis of the benzene ring of PN resin [30]. It was shown that the polymer skeleton structure has been seriously damaged at 690 °C. The volatile products evolving from the last pyrolysis step at 799 °C are reflected in Fig. 4(4). CO_2, CO and CH_4 are still evolved probably by

Table 2
Parameters under curve of each separated peak at 10 °C/min.

Heating rate (°C/min)	Peak 1		Peak 2	
	Peak center (°C)	Percent area Under curve (%)	Peak center (°C)	Percent area Under curve (%)
10	560	32.69	670	67.31

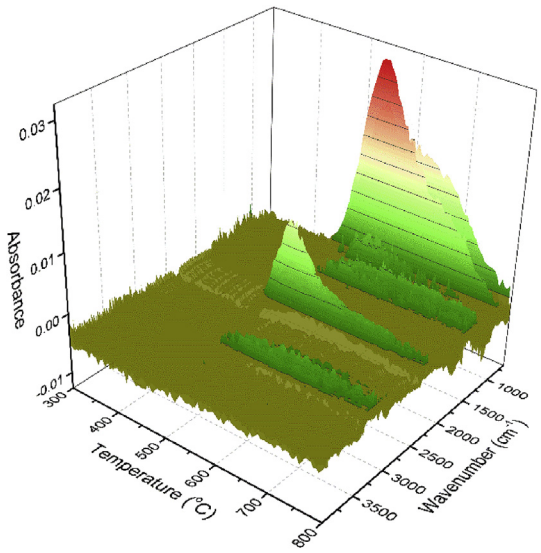

Fig. 3. 3D FTIR diagram of PN resin pyrolysis with a heating rate of 10 °C/min.

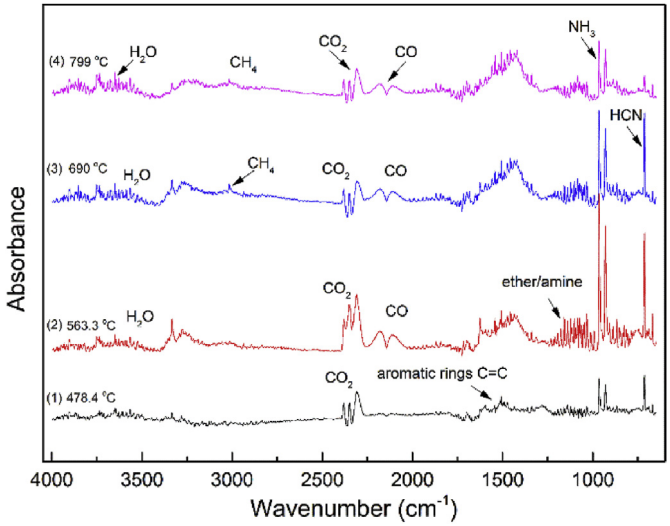

Fig. 4. FTIR spectra of volatile products at representative temperature of PN resin.

the pyrolysis process of aromatic char at high temperature. In a summary, the dominant components of the volatile products during pyrolysis of sample including NH_3, HCN, CH_4, CO_2, CO, H_2O and aromatic ring.

3.3. TG-MS analysis of gas products

Fig. 5 shows the distributions of all the fragment ions by full scanning mode (scan (1–160)) at 560.5 °C and 700.8 °C under the heating rate of 10 °C/min. The National Institute of Science and Technology (NIST) database was employed to identified the volatile compounds [35]. As shown in Fig. 5, it can be observed that the intensity of these MS signals has varied and was dependent on the concentration of the corresponding species in the gas mixture (released during the thermal pyrolysis). The molecular structure of resin is damaged more seriously at 700.8 °C, and thus the sample at 700.8 °C present spectra with more MS signals compared to ones at 500.5 °C. Meanwhile, the MS spectra are very complex due to fragmentation in many mass ions. The signals of the main volatile products were identified as follows: H_2O^+ ($m/z = 18$), CH_4^+ ($m/z = 16$), NH_3^+ ($m/z = 17$), HCN^+ ($m/z = 27$), CO^+ ($m/z = 28$), CO_2^+ ($m/z = 44$), $C_6H_6^+$ ($m/z = 78$).

The evolution curves of major gaseous products, tracked by the selected ion recording mode, are plotted in Fig. 6a–j. CH_4 is the main hydrocarbon product in PN pyrolysis. Fig. 6a presents the evolution curve of CH_4. As shown in Fig. 5a, CH_4 is mainly generated in the temperature range from 520 °C to 800 °C, and evolving content reaches maximum at nearly 590 °C. It is well known that PN resin have high levels of aromatic and heterocycle ring structure within the cross-linked network. Compared to aliphatic structure, the pyrolysis of aromatic and heterocycle structures needs more energy or higher temperature. CH_4 is generated from the breakage of the benzene ring, secondarily pyrolysis of heterocycle structure (triazine ring or phthalocyanine structure), and polycondensation reaction of aromatic molecules [30]. In fact, the destruction of these structures usually takes a long time and requires a wide temperature range. Therefore, there are different chemical reactions at 520 °C–800 °C with the change of temperature, and the emission of CH_4 may be caused by the distinct reaction at different temperature, which may be the reason why CH_4 still maintains a relatively high content after 600 °C.

Fig. 6b and Fig. 6d depicts the release history of NH_3 and HCN, respectively. NH_3 is mainly released at temperature of 520–700 °C and evolving content reaches maximum at nearly 580 °C. The peak was mainly derived from fragmentation of triazine ring or isoindoline structure. HCN is formed in a relatively wide temperature range (460–800 °C) with a "blunt" peak at ~ 600 °C. In the low temperature region, the released of HCN can be interpreted by the removal of unreacted cyanogen group on benzene ring. Meanwhile, because of the planar conjugate structure of triazine rings and phthalocyanine rings and their high thermal stability, the pyrolysis of these structure occurs at higher temperature, which occurs in a wide temperature range and may produce by-products such as NH_3 and HCN.

The evolution curve of H_2O is shown in Fig. 6c. It is worth noting that moisture will be generated in two stages. The first stage occurs at low temperature (<500 °C), probably owing to the absorbed water within PN resin. The evolution of H_2O at high temperature (>500 °C) is usually associated with phenolic OH groups [30]. Some unreacted OH in sample will be removed from the benzene ring with the increasing temperature. Additionally, owing to the different bond energy of C–OH and C–O, the evolution curve of pyrolysis H_2O occurs in wide temperature [36].

The evolution of CO and CO_2 as the temperature increased is shown in Fig. 6e and Fig. 6f, respectively. In the argon atmosphere, two peaks of CO release were found at 500–800 °C that was mainly

Table 3
Gas species and functional groups characterized by the wavenumber range in the present study.

Detected gas	Functional group	Vibration	Wavenumber(cm^{-1})	References
H_2O	O—H	stretch	4000–3500	[29]
	H—O—H	bending	1875–1275	[29]
CH_4	C—H	stretch	3000–2800	[30]
CO_2	C=O	stretch	2400–2240	[31]
	C=O	bending	736–605	[31]
CO	C—O	stretch	2240–2050	[32]
Aromatics	C=C and benzene skeleton	stretch	1690–1450	[24]
HCN	C—H	bending	815–615	[33]
	N≡CH	stretch	3312	[35]
NH_3	N—H	stretch	3340	[34]
	N—H	bending	966, 927	[34]

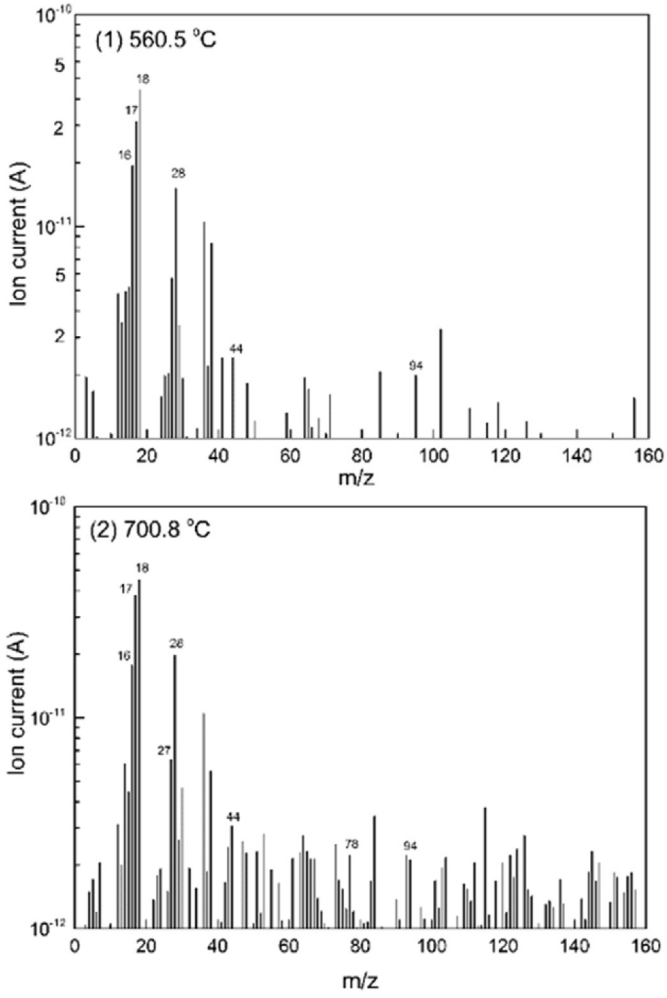

Fig. 5. MS spectra of thermal pyrolysis products at (1) 560.5 °C and (2) 480 °C at the heating rate of 10 °C/min.

caused by the breakage of oxygen containing functional groups [32]. In the first peak at lower temperature (~580 °C), the release of CO might be mainly contributed by the thermal pyrolysis of phenol group. In the second peak at higher temperature (~720 °C), the release of CO was mainly contributed by the formation of biphenyl and oxygen-containing heterocyclic compounds [24,31,32]. CO_2 is generated from low temperature to high temperature (500–800 °C). With the increasing temperature, the ion current of CO_2^+ also increases and the content reaches maximum at around 550 °C. It also presents a shoulder in the evolution curve of CO_2 after 650 °C. In fact, the production of CO and CO_2 is a comprehensive competition process. For example, CO can produce through the Boudouard reaction (reaction (1)) [37]. While CO_2 can also dissociate into CO and O_2 through the reaction (2) [38].

$$C(s)+CO_2 \rightarrow 2CO \quad (1)$$

$$CO_2 \rightarrow CO+0.5O_2 \quad (2)$$

As shown in Fig. 6g, with the increasing temperature, the release intensity of benzene rapidly increases and the content reaches maximum at around 580 °C. It is commonly known that PN resin has abundant aromatic structures, and because of the steady state of benzene ring, it is difficult to break for aromatic nucleus bond at lower temperature. However, the bridged bond (such as C—O—C) could be relatively labile with the increasing temperature. When the temperature is higher than 700 °C, the free benzene can recombine to form polyphenyl or further carbonization which will finally lead to the formation of char.

3.4. The possible thermal pyrolysis mechanism of PN resin

Based on the TG-MS-FTIR experiment analysis above in argon atmosphere, the thermal pyrolysis mechanism of PN resin under non-oxidizing gaseous environment can be proposed. The possible structure of products formed during pyrolysis of sample are shown in Scheme 2. Firstly, as shown in Scheme 2, in the beginning of pyrolysis, little unreacted cyano groups, phenolic hydroxyl groups and C—O—C, which are the labile bonds in the polymer, could be easily removal under heating. A variety of small molecules could produce first, such as HCN, NH_3, H_2O and benzene etc. Secondly, as shown in the results of FTIR and MS data, the volatiles become more complex with temperature increasing. The main pyrolysis stage of resin was ranged from 500 °C to 650 °C, with concomitant ring-opening of heterocyclic compound and decomposition of benzene ring. Moreover, the heterocyclic structures can availably combine benzene ring and heteroatoms together to form chars easily with graphitic structures [39]. Zhang et al. [40] reported a superior electromagnetic interference shielding carbon foam through direct carbonization of PN-based polymer foam, the result indicate that the high graphitic carbonaceous species and intrinsic nitrogen-containing structure contribute the high electromagnetic interference shielding effectiveness properties.

According to previous papers, the thermal pyrolysis behavior of high-performance polymers, such as cyanate eater [41,42], polybenzoxazines [39] and phenol-formaldehyde resin [43] were investigated by TGA-FTIR or Py-GC-MS. The experimental evidence presented thus far suggests a better understanding on why the PN resin has superior thermal stability compared to other resins. As is known, PN resin contain a substantial proportion of aromatic and

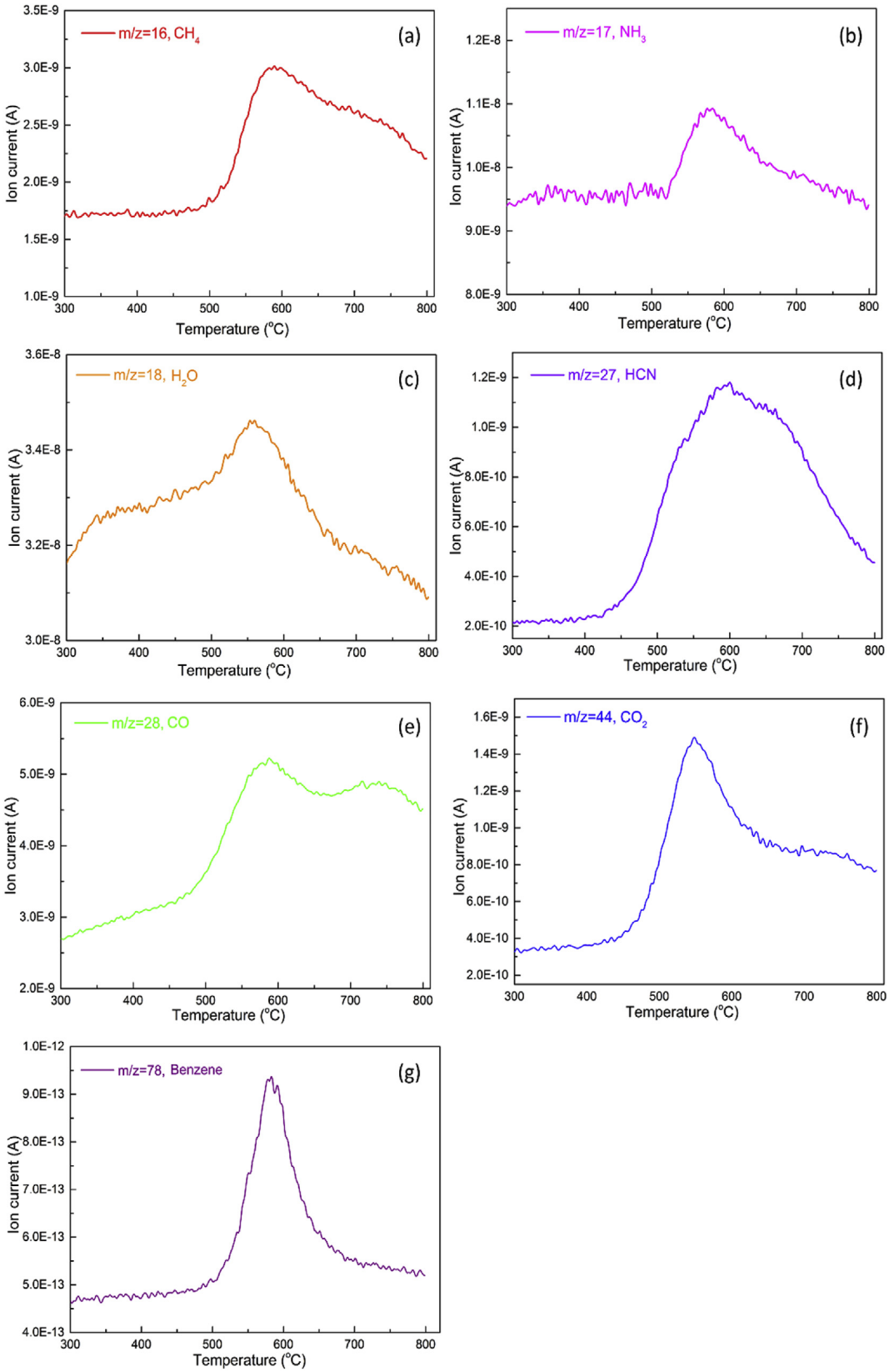

Fig. 6. The ion current of the major gaseous species released from PN resin thermal pyrolysis in argon atmosphere.

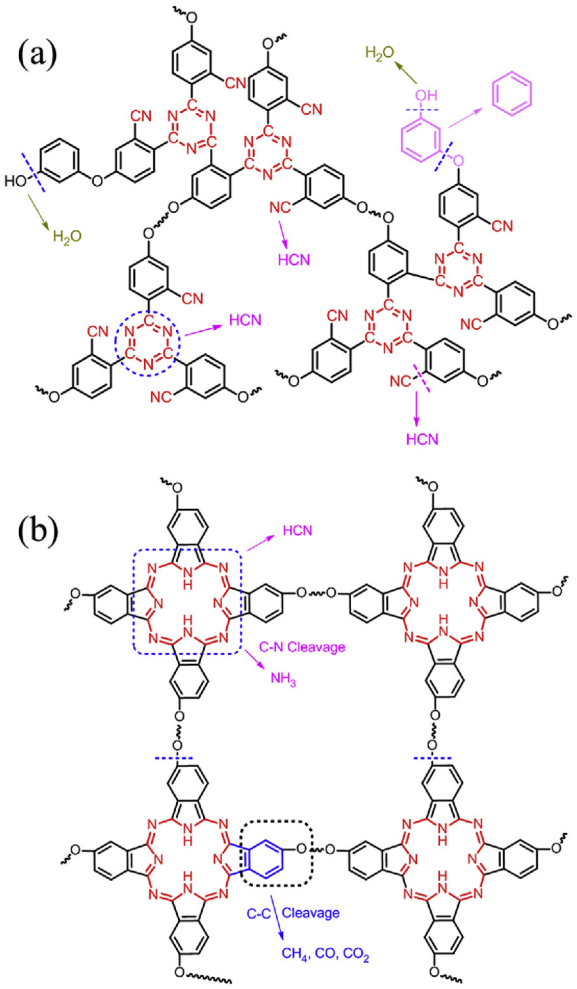

Scheme 2. The possible pyrolysis mechanism of PN resin. (a) Triazine structure. (b) phthalocyanine structure.

heteroaromatic rings (such as phthalocyanine ring and triazine ring), these structures have superior thermal stability due to the resonance stabilization. Factors such as rigid groups, bulky groups and high crosslink density could increase the thermal stability of polymer. For PN resin, a stiffer chain will lead to slower thermal movement at higher temperature and thus greater thermal stability. Moreover, hydrogen bonding, polar interaction and van der Waals forces should be considered to further improve the stability of PN resin. However, the lower bond dissociation energy of C—O—C could affect the thermal stability of PN resin. For example, Zhong et al. [44] simulated the pyrolysis process of phenolic resin by reactive force field molecular dynamics simulation. The results suggested that the formation of phenoxyl radicals can reduced the stability of benzene ring and damaged backbone of phenolic resin accompanying with the release of gaseous products (CO, CO_2 etc.).

4. Conclusions

In this study, thermal pyrolysis characteristic of PN resin under inert atmosphere was investigated by TG-MS-FTIR. For PN resin, two-step pyrolysis mechanism is proposed and the maximum mass loss rate occurred at about 580 °C. The main volatile products from thermal pyrolysis of PN resin, identified by TG-MS-FTIR analysis, revealed H_2O, NH_3, HCN, CH_4, CO_2, CO. In the range of 450—650 °C, the possible pyrolysis mechanism may firstly occur in the elimination of phenyl pendant group and the breakage of other weaker bonds (such as C—O—C). At temperature above 650 °C, resin occur carbonization and the mass loss rate of sample decreased. The results of this study provide useful information for understanding the pyrolysis mechanism of PN resin and for designing high-performance resin with better flame retardant properties.

References

[1] P.M. Lipic, F.S. Bates, M.A. Hillmyer, Nanostructured thermosets from self-assembled amphiphilic block copolymer/epoxy resin mixtures[J], J. Am. Chem. Soc. 120 (35) (1998) 8963—8970.
[2] DerJang Liaw, ChangSik Ha, JuinYih Lai, KueirRarn Lee, YingChi Huang, KungLi Wang, Advanced polyimide materials: synthese, physical properties and applications, Prog. Polym. Sci. 37 (2012) 907—974.
[3] Y.L. Liu, C.I. Chou, High performance benzoxazine monomers and polymers containing furan groups, J. Polym. Sci., Part A: Polym. Chem. 43 (2010) 5267—5282.
[4] M.K. Kolel-Veetil, D.D. Dominguez, T.M. Keller, Dendritic networks containing polyhedral oligomeric silsesquioxane (POSS) and carborane clusters, J. Polym. Sci., Part A: Polym. Chem. 46 (2010) 2581—2587.
[5] D. Augustine, K.P. Vijayalakshmi, R. Sadhana, D. Mathew, C.P.R. Nair, Hydroxyl terminated PEEK-toughened epoxy—amino novolac phthalonitrile blends — synthesis, cure studies and adhesive properties, Polymer 55 (23) (2014) 6006—6016.
[6] S.B. Sastri, T.M. Keller, Phthalonitrile cure reaction with aromatic diamines, J. Polym. Sci., Part A: Polym. Chem. 36 (2015) 1885—1890.
[7] K. Zeng, G. Yang, Phthalonitrile Matrix Resins and Composites, 2012.
[8] A.P. Mouritz, E. Gellert, P. Burchill, K. Challis, Review of advanced composite structures for naval ships and submarines, Compos. Struct. 53 (2001) 21—42.
[9] Y. Liu, J. Hu, R. Li, C. Li, B. Liang, Y. Liu, W. Peng, K. Zeng, G. Yang, A prospective partial bio-based diamine-adenine-monomer platform for high performance polymer: a case study on phthalonitrile resin, Polym. Degrad. Stab. 167 (2019) 114—123.
[10] T.M. Keller, The Synthesis of a New Class of Polyphthalocyanine Resins, 1980.
[11] D.D. Dominguez, H.N. Jones, T.M. Keller, The effect of curing additive on the mechanical properties of phthalonitrile-carbon fiber composites, Polym. Compos. 25 (2010) 554—561.
[12] D.D. Dominguez, T.M. Keller, Low-melting phthalonitrile oligomers: preparation, polymerization and polymer properties, High Perform. Polym. 18 (2006) 283—304.
[13] M. Laskoski, D.D. Dominguez, T.M. Keller, Synthesis and properties of a bisphenol A based phthalonitrile resin, J. Polym. Sci., Part A: Polym. Chem. 43 (2010) 4136—4143.
[14] Y. Ping, S. Ji, J. Hu, X. Hu, Z. Ke, Y. Gang, Systematic Study on Highly Efficient Thermal Synergistic Polymerization Effect between Alicyclic Imide Moiety and Phthalonitrile: Scope, Properties and Mechanism, vol. 102, 2016, pp. 266—280.
[15] T. Fu, X. Zhao, L. Chen, W.S. Wu, Q. Zhao, X.L. Wang, D.M. Guo, Y.Z. Wang, Bioinspired color changing molecular sensor toward early fire detection based on transformation of phthalonitrile to phthalocyanine[J], Adv. Funct. Mater. 29 (8) (2019) 1806586.
[16] D. Augustine, D. Mathew, C.P.R. Nair, Phenol-containing phthalonitrile polymers — synthesis, cure characteristics and laminate properties, Polym. Int. 62 (2013) 1068—1076.
[17] D. Wu, Y. Zhao, Z. Ke, Y. Gang, A novel benzimidazole-containing phthalonitrile monomer with unique polymerization behavior, J. Polym. Sci., Part A: Polym. Chem. 50 (2015) 4977—4982.
[18] J. Hu, Y. Liu, Y. Jiao, S. Ji, R. Sun, P. Yuan, K. Zeng, X. Pu, G. Yang, Self-promoted phthalimide-containing phthalonitrile resins with sluggish curing process and excellent thermal stability, RSC Adv. 5 (2015) 16199—16206.
[19] H. Guo, Z. Chen, J. Zhang, X. Yang, Z. Rui, X. Liu, Self-promoted curing phthalonitrile with high glass transition temperature for advanced composites, J. Polym. Res. 19 (2012) 9918.
[20] X. Li, J. Wang, Y. Sun, D. Zhang, N. Zhu, L. Jing, The effect of thermal treatment on the decomposition of phthalonitrile polymer and phthalonitrile-polyhedral oligomeric silsesquioxane (POSS) copolymer, Polym. Degrad. Stab. 156 (2018) 279—291.
[21] C. Liu, J. Wang, E. Lin, L. Zong, X. Jian, Synthesis and properties of phthalonitrile-terminated oligomeric poly(ether imide)s containing phthalazinone moiety, Polym. Degrad. Stab. 97 (2012) 460—468.
[22] B. Liang, J. Hu, P. Yuan, C. Li, R. Li, Y. Liu, K. Zeng, G. Yang, Kinetics of the pyrolysis process of phthalonitrile resin, Thermochim. Acta 672 (2019) 133—141.
[23] G. Lisa, Y. Yoshitake, T. Michinobu, Thermal degradation of some ferrocene-containing poly(aryleneethynylene)s, J. Anal. Appl. Pyrolysis 120 (2016). S1034490035.
[24] L. Jiao, H. Xiao, Q. Wang, J. Sun, Thermal degradation characteristics of rigid polyurethane foam and the volatile products analysis with TG-FTIR-MS, Polym. Degrad. Stab. 98 (2013) 2687—2696.
[25] E. Hamciuca, M. Cazacu, M. Ignat, G. Zarnescu, Polyimide—polydimethylsiloxane copolymers containing nitrile groups, Eur. Polym. J. 45 (2009) 182—190.

[26] F. Mustata, N. Tudorachi, I. Bicu, The kinetic study and thermal characterization of epoxy resins crosslinked with amino carboxylic acids, J. Anal. Appl. Pyrolysis 112 (2015) 180–191.
[27] J. Wang, J. Hu, Z. Ke, Y. Gang, Preparation of self-promoted hydroxy-containing phthalonitrile resins by in situ reaction, RSC Adv. 5 (2015) 105038–105046.
[28] SergeyVyazovkin, Kinetic concepts of thermally stimulated reactions in solids: a view from a historical perspective, Int. Rev. Phys. Chem. 19 (2000) 45–60.
[29] Y.A. Opata, J.C. Grivel, Synthesis and thermal decomposition study of dysprosium trifluoroacetate, J. Anal. Appl. Pyrolysis 132 (2018). S1035497363.
[30] Y. Huang, H. Liu, H. Yuan, X. Zhuang, S. Yuan, X. Yin, C. Wu, Association of chemical structure and thermal degradation of lignins from crop straw and softwood, J. Anal. Appl. Pyrolysis 134 (2018) 25–34.
[31] M. Brebu, T. Tamminen, I. Spiridon, Thermal degradation of various lignins by TG-MS/FTIR and Py-GC-MS, J. Anal. Appl. Pyrolysis 104 (2013) 531–539.
[32] J. Yang, H. Chen, W. Zhao, J. Zhou, TG–FTIR-MS study of pyrolysis products evolving from peat, J. Anal. Appl. Pyrolysis 117 (2016) 296–309.
[33] Z. Wang, P. Lv, H. Yuan, K. Hu, Thermal degradation study of intumescent flame retardants by TG and FTIR: melamine phosphate and its mixture with pentaerythritol, J. Anal. Appl. Pyrolysis 86 (2009) 207–214.
[34] X. Li, L. Chen, X. Dai, Q. Mei, G. Ding, Thermogravimetry–Fourier transform infrared spectrometry–mass spectrometry technique to evaluate the effect of anaerobic digestion on gaseous products of sewage sludge sequential pyrolysis, J. Anal. Appl. Pyrolysis 126 (2017) 288–297.
[35] F.W. Olver, D.W. Lozier, R.F. Boisvert, C.W. Clark, NIST Handbook of Mathematical Functions, 2010.
[36] E. Jakab, F. Till, G. Várhegyi, Thermogravimetric-mass spectrometric study on the low temperature oxidation of coals, Fuel Process. Technol. 28 (2015) 221–238.
[37] L.G. Zheng, E. Furimsky, Assessment of coal combustion in O2+CO2 by equilibrium calculations, Fuel Process. Technol. 81 (2003) 23–34.
[38] P. Glarborg, L.L.B. Bentzen, Chemical effects of a high CO2 concentration in oxy-fuel combustion of methane, Energy Fuel. 22 (2008) 291–296.
[39] H. Zhang, G. Wu, R. Zhu, Q. Ran, G. Yi, Study on the thermal degradation behavior of sulfone-containing polybenzoxazines via Py-GC-MS, Polym. Degrad. Stab. 111 (2015) 38–45.
[40] L. Zhang, M. Liu, S. Roy, E.K. Chu, K.Y. See, X. Hu, Phthalonitrile-Based Carbon Foam with High Specific Mechanical Strength and Superior Electromagnetic Interference Shielding Performance, 2016.
[41] Q. Lin, L. Bei, L. Qu, C. Fang, Z. Chen, Direct preparation of carbon foam by pyrolysis of cyanate ester resin at ambient pressure, J. Anal. Appl. Pyrolysis 104 (2013) 714–717.
[42] M.L. Ramirez, R. Walters, R.E. Lyon, E.P. Savitski, Thermal decomposition of cyanate ester resins, Polym. Degrad. Stab. 78 (2002) 73–82.
[43] H. Jianga, S. Wu, Z. Yuan, Z. Hu, R. Wu, Q. Liu, The pyrolysis mechanism of phenol formaldehyde resin, Polym. Degrad. Stab. 97 (2012) 1527–1533.
[44] Y. Zhong, X. Jing, S. Wang, Q.X. Jia, Behavior investigation of phenolic hydroxyl groups during the pyrolysis of cured phenolic resin via molecular dynamics simulation, Polym. Degrad. Stab. 125 (2016) 97–104.